Rainfall erosivity in interrill areas

Amina Nouhou Bako, Frédéric Darboux, François James, Carine Lucas

Rainfall erosivity in interrill areas: insights about the choice of an erosive factor

A. Nouhou Bako[a,b]*, F. Darboux[a,c], F. James[b] and C. Lucas[b]
[a]URSOLS, INRA, F-45075 Orléans, France.
[b]Institut Denis Poisson, Université d'Orléans, Université de Tours, CNRS, Route de Chartres, BP 6759, 45067 Orléans cedex 2, France.
[c]Presently at: Université de Lorraine, INRA, LSE, F-54000 Nancy, France.

March 18, 2019

Abstract

Defining a suitable erosive factor for interrill erosion has been a long-going discussion that was not resolved by experimental results. In this paper, by using computational fluid simulations of individual raindrop impacts, the relevance of four erosive factors was assessed for a range of soil resistance, rainfall type and water layer depth. Computation results show that the erosivity exponent associated to the erosive factors had a very low sensitivity to soil resistance. This confirms the common practice of separating rainfall erosivity from soil erodibility. The erosivity exponent was found to be very sensitive to the rainfall type. Therefore, an universal exponent could not be found, its value depending on the rainfall type. As a result of the balance between the shear stress development and the protective effect of the water layer, the soil detachment rate was maximum for a specific water depth. This supports to better account for the water layer depth in erosion models. Overall, the computational approach shows that the choice of an erosive factor may not be of practical importance. It also encourages for new experimental designs, able to evaluate soil detachment by raindrops — and not only the amount of splashed soil.

Keywords: Raindrop, detachment, shear stress, computer simulation, water layer depth, erosivity

1 Introduction

Raindrop detachment is the first process to take place in interrill erosion. It has been defined by Ellison (1944) as the separation of the soil particles from the initial soil matrix due to rain. It is caused by the shear stress created by the raindrop impacts at the soil surface. Raindrop detachment is essential before soil particles can then be splashed, transported in overland flow, etc.

The amount of soil detached by raindrops was studied experimentally, leading to many formulas predicting the amount of soil detached by rain in the context of interrill erosion (Rose et al., 1983; Bradford et al., 1987; Sharma et al., 1993; Gabet and Dunne, 2003; Mouzai and Bouhadef, 2011; Brodowski, 2013). In these soil detachment formulas, rainfall erosivity, i.e. the rainfall ability to cause soil detachment, is expressed by an erosive factor. The rainfall intensity I (Nanko et al., 2016; Nearing et al., 1989; Kinnell, 1982; Meyer, 1981; Cuomo et al., 2016; Fernández-Raga et al., 2017) and the rainfall kinetic energy E_k (De Roo et al., 1996; Morgan et al., 1998; Sharma et al., 1993; Usón and Ramos, 2001; Assouline, 2009) have been the most widely used erosive factors (Shin et al., 2016; Nearing et al., 2017; Yin et al., 2017). Many other erosive factors have been

*Corresponding author: A. Nouhou Bako, URSOLS, INRA, Centre de recherche Val de Loire, F-45075 Orléans Cedex 2, France. Email: aminam_nb@yahoo.fr.
Frédéric Darboux: Frederic.Darboux@inra.fr
François James: francois.james@math.cnrs.fr
Carine Lucas: carine.lucas@univ-orleans.fr

of significant use, like the rainfall momentum M, the momentum multiplied by the raindrop diameter (MD), while some other were proposed but rarely used, such as the kinetic energy divided by the raindrop diameter (E_k/D) and the kinetic energy divided by the square of the raindrop diameter (E_k/D^2) (Salles and Poesen, 2000; Salles et al., 2000; Sanchez-Moreno et al., 2012; Goebes et al., 2014; Nanko et al., 2016).

Currently, there is no consensus about the most suitable erosive factor, as exemplified by papers comparing them (Salles et al., 2000; Usón and Ramos, 2001; Goebes et al., 2014). Indeed, the extensive number of available erosive factors casts doubt about our understanding of the detachment process. It also questions the capability of the various erosive factors to describe properly the rainfall ability to cause soil detachment. Moreover, even if it has been documented that both the shear stress (Hartley and Julien, 1992; Wang and Wenzel, 1970; Nouhou Bako et al., 2016) and soil detachment (Mutchler and Young, 1975; Torri and Sfalanga, 1986; Dunne et al., 2010) caused by the raindrops depend on the water layer depth, most of the soil detachment formulas (Nearing et al., 1989; Sharma et al., 1993; Rose et al., 1983; Smith and Wischmeier, 1957; Brodowski, 2013) were defined for un-inundated conditions only (i.e. a null water depth). Hence, these formulas and their erosive factors may not be suitable for inundated conditions (puddles, overland flow). The soil detachment formulas accounting for the effect of the water layer thickness include either an erosivity exponent scaling the erosive factor, or a function describing the effect of the water layer depth on the soil detachment. The present work considers these two approaches.

Numerical studies of the raindrop shear stress have been carried out by several authors (Hartley and Alonso, 1991; Hartley and Julien, 1992; Wang and Wenzel, 1970). Recently, Nouhou Bako et al. (2016) obtained a complete description of the shear stress created by a single raindrop impacting a water layer using a fluid mechanics software solving the Navier–Stokes equations. Computations of shear stress were successfully used in the case of flow detachment (Sanford and Maa, 2001).

The present paper considers raindrops impacting a water layer covering the soil surface, a common situation in interrill erosion. Through computer simulations similar to Nouhou Bako et al. (2016), it relates the shear stress caused by rain to the detachment of soil. The main goal is to evaluate the relevance of four previously-used erosive factors (I, E_k, M, and MD). Additional goals are (1) to assess the dependence of the erosive factors to water depth, rainfall drop size distribution, and soil resistance to shear stress, (2) to test the validity of the classical segmentation between rainfall erosivity and soil erodibility, and (3) to have a critical look at how erosion models and experiment designs account for soil detachment and water depth.

2 Materials and Methods

The relationships between detachment rates and erosive factors were established based on three successive stages:

1. Calculation of the amount of soil detached by a single raindrop impacting a soil surface covered by a water layer, using computational fluid dynamics simulations (Section 2.1).

2. Calculation of the detachment rates caused by a rainfall, for a range of water layer depths, accounting for the raindrop size distribution of the rainfall (Section 2.2).

3. Evaluation of the relationships between detachment rates and erosive factors, either through an erosivity exponent altering the erosive factor value, or through a function describing directly the effect of the water layer depth on the soil detachment (Section 2.3).

2.1 Soil Detachment for a Single Raindrop

The impact of a single raindrop on a soil surface covered by a water layer was calculated by computational fluid dynamics simulations.

The raindrop impact causes a shear stress $\tau(r,t)$ (Pa) that is postulated to extend radially with time. This shear stress is related to the erosion rate using:

$$E(r,t) = M_c(\tau(r,t) - \tau_c) \tag{1}$$

where $E(r,t)$ ($\mathrm{kg.m^{-2}.s^{-1}}$) is the local rate of erosion, M_c ($\mathrm{s.m^{-1}}$) is an empirical constant, and τ_c (Pa) is the critical shear stress needed to detach soil particles. Equation (1) is identical to a law commonly used for flow detachment (Lang et al., 1989; McLean, 1985; Ariathurai, 1974) and was chosen because of its simplicity. It expresses that a minimal shear stress should be applied to the soil surface to get detached particles, and that, above this threshold, the amount of detached particles is proportional to the applied shear stress.

The simulations allowed for the calculation of the shear stress $\tau(D,h)(r,t)$ created at the soil surface by a raindrop of diameter D (mm) and velocity V_f ($\mathrm{m.s^{-1}}$) impacting vertically a horizontal water layer of thickness h (mm). Because raindrops were considered at terminal velocity in the air, the direct relation between their diameter D and their velocity V_f (see Equation (7) below) allowed to remove the dependency in V_f in the following.

For each value of D, the simulations were carried out for various depths h of the water layer. For each set of D and h values, the shear stress has a maximum extent radius $R_{max}(D,h)$ (mm) and an associated duration $t_{max}(D,h)$ (s). For a complete description of the calculation of the shear stress, the reader is referred to Nouhou Bako et al. (2016).

The total soil detachment $d_s(D,h)$ (kg) caused by a single raindrop was then calculated by integrating Equation (1) in space and time using cylindrical coordinates:

$$d_s(D,h) = 2\pi M_c \int_0^{t_{max}(D,h)} \int_0^{R_{max}(D,h)} (\tau(D,h)(r,t) - \tau_c) r dr dt. \tag{2}$$

In this description, the critical shear stress τ_c is the only variable depending on the soil properties. Its value ranges from 0.02 to 0.74 Pa according to the literature review of Houwing (1999).

2.2 Soil Detachment for a Rainfall

A rainfall can be characterized by the distribution of the diameters of its drops (or drop size distribution, DSD). The DSD is characterized by $N_v(D)$, the number of drops for each diameter D (mm) in a unit volume of air (i.e. 1 $\mathrm{m^3}$). Numerous laws defining the DSD of natural rainfalls have been published (Torres et al., 1994; Cugerone and Michele, 2015). In order to evaluate the effect of different types of rainfall onto the soil detachment, three usual DSD laws were selected:

- The Marshall and Palmer (1948) law given by:

$$N_v(D) = 8000 \exp\left(-4.1\, I^{-0.21} D\right), \tag{3}$$

  where I is the rainfall intensity ($\mathrm{mm.h^{-1}}$).

- The Gamma law of Ulbrich (1983) for a stratiform rain, which reads:

$$N_v(D) = 6.4 \times 10^{10} D^{4.65} \exp\left(-\frac{8.32}{0.114\, I^{0.11}} D\right). \tag{4}$$

- The Lognormal law of Feingold and Levin (1986):

$$N_v(D) = \frac{172\, I^{0.22}}{\sqrt{2\pi}(\ln 1.43) D} \exp\left(-\frac{\ln^2\left(\frac{D}{0.72\, I^{0.23}}\right)}{2\ln^2 1.43}\right). \tag{5}$$

While the DSD gives the distribution in diameter of the raindrops in a volume of air, the present issue concerns the drops reaching the ground, which involves the falling velocity of each drop diameter. Following on Hall and Calder (1993) and Brodie and Rosewell (2007), the density of raindrops reaching the ground was estimated with

$$N_a(D) = N_v(D) V_f(D) \tag{6}$$

where $V_f(D)$ is the terminal velocity of the raindrop (m.s^{-1}) and is estimated with the formula of Uplinger (1981):

$$V_f(D) = 4.854\, D \exp(-0.195\, D), \tag{7}$$

where D is in millimeter. While this relationship was initially defined for a raindrop diameter up to 5 mm, in this study it was applied up to 6 mm (see below).

Because the actions of raindrops are mostly independent from one another regarding the detachment process (Nouhou Bako et al., 2017; Salles et al., 2000; Sharma et al., 1993; Gilley et al., 1985), the detachment caused by a rainfall can be estimated through the summation of the quantity of soil detached by its individual raindrops. So, the amount of soil detached by rain $D_s(h)$ (kg.m^{-2}.s^{-1}) for a water layer of depth h was calculated as:

$$D_s(h) = \int_{D_{min}}^{D_{max}} d_s(D,h) N_a(D) dD, \tag{8}$$

where h is the water layer depth covering the soil surface, D_{min} and D_{max} are the smallest and largest drop diameters considered, respectively, and $d_s(D,h)$ is the soil detachment caused by a raindrop of diameter D for the given water layer depth h, as given by Equation (2).

2.3 Rainfall Detachment, Erosive Factors and Water Depth

Rainfall erosivity can be expressed through various erosive factors. In this study, the four most used erosive factors were considered:

- the rainfall intensity I,
- the kinetic energy E_k of the rainfall,
- the momentum M of the rainfall,
- the product of the momentum by the diameter MD.

The rainfall intensity I was first set in the DSD law (i.e. Equations (3), (4) or (5)), and then the other erosive factors were calculated with the formula of Salles et al. (2000):

$$Er_{\gamma,\eta} = C_{\gamma,\eta} \sum_{i=1}^{N} D_i^{\gamma} V_{fi}^{\eta} \tag{9}$$

where $Er_{\gamma,\eta}$ is an erosive factor of the rainfall, γ and η are integers, and $C_{\gamma,\eta}$ is a constant. The number N is the total number of raindrops at the ground, per second and per square meter, given by $N = \int_{D_{min}}^{D_{max}} N_a(D) dD$. More precisely, considering an area of 1 m^2 and a duration of 1 s for the computation of $C_{\gamma,\eta}$ (Salles et al., 2000),

- $Er_{3,2}$ is the kinetic energy of rainfall E_k with $C_{3,2} = \frac{\pi \rho_l}{12}$,
- $Er_{3,1}$ is the momentum M with $C_{3,1} = \frac{\pi \rho_l}{6}$,
- $Er_{4,1}$ is the momentum multiplied by the diameter MD with $C_{4,1} = \frac{\pi \rho_l}{6}$,

where ρ_l is the water density.

The amount of soil detached by rain can be related to these erosive factors through:

$$D_s(h) = A \times (Er_{\gamma,\eta})^{B(h)}. \tag{10}$$

In Formula (10), A is the coefficient of soil detachability and depends only on soil properties. The present work did not address this soil detachability coefficient because the calculation of the raindrop shear stress was

performed on a non-erodible rigid surface. The study focused on the erosivity exponent $B(h)$ in Formula (10). The erosivity exponent $B(h)$ expresses how the soil detachment evolves with the erosive factor of the rain, and how the water depth affects this evolution. Previous works have used such a power law to relate the soil detachment to the rainfall erosivity (Meyer, 1981; Nearing et al., 1989; Smith and Wischmeier, 1957; Salles et al., 2000), and preliminary tests showed that this power law gave better fits with our results than linear and exponential laws.

In many models, $B(h)$ is calibrated independently of the soil properties (the soil properties being included in A only). It is obvious from Formula (10) that the detachment is more sensitive to the erosive factor than to the detachability for $B(h) > 1$; and vice-versa for $B(h) < 1$. In the present work, soil detachment $D_s(h)$ (calculated by Formula (8)) and erosive factors $Er_{\gamma,\eta}$ (calculated by Formula (9)) were first evaluated independently to get sets of $D_s(h)$ and $Er_{\gamma,\eta}$ values. Then regressions over Formula (10) allowed to estimate coefficients A and $B(h)$.

For the special case $B(h) = 1$, the detachment is linearly proportional to the erosive factor and does not depend on the depth of the water layer. Some models, such as LISEM (De Roo et al., 1996) and EUROSEM (Morgan et al., 1998; Gumiere et al., 2009), make use of this special case. They separate the erosive factor and the effect of the water layer by defining the amount of soil detached by rain D_s as:

$$D_s(h) = K \times G(h) \times Er_{\gamma,\eta}, \tag{11}$$

with K the soil erodibility coefficient (Morgan et al., 1998) and $G(h)$ a function describing the effect of the water layer depth on the soil detachment. Depending on the $G(h)$ formulation, the water layer could limit or hasten soil detachment. As for the previous model, regressions over Formula (11) were carried out to define $G(h)$ from computations using (8) and (9).

2.4 Computations and Analysis

The computations and result analysis were carried out in four successive steps:

1. For each drop of diameter D impacting a water layer of depth h, the time and space evolution of the shear stress $\tau(D,h)(r,t)$ was simulated by the *Gerris* software (version 2016-12-06). *Gerris* is a computational fluid dynamics software solving the Navier–Stokes equations (Popinet, 2003). Written in C, *Gerris* is free and open-source (`http://gfs.sourceforge.net/`, 2017-12-11). Because of the axial symmetry of the problem, cylindrical coordinates were used, allowing for faster simulations.

2. Using the Scilab software (`https://www.scilab.org`, 2017-12-12), the amount of soil detached by a raindrop $d_s(D,h)$ was calculated by solving numerically Equation (2) considering a predefined shear stress threshold τ_c. Four threshold values (τ_c=0, 0.25, 1 and 5 Pa) were used. Note that, while the first three values were in the experimentally-observed range given by Houwing (1999), the fourth one ($\tau_c = 5$ Pa) is very large and clearly out of the natural range. Such a large value was included for the only purpose of bringing out a potential effect of the shear threshold.

3. The amount of soil detached by a rainfall $D_s(h)$ was calculated by Formula (8), using Scilab. The $D_s(h)$ calculation was carried out for various combinations of rainfall intensity, DSD law, and water layer depth h. Raindrop diameters ranging from D_{min}= 0.5 mm (because smaller raindrops do not cause any significant detachment (Moss and Green, 1983)) to D_{max}= 6 mm (because larger raindrops are extremely rare — see Low and List (1982) and Equations (3), (4) and (5)) were taken into account. Note that this maximum diameter is a bit larger that the one defined by Low and List (1982) in Equation (7) (i.e. 5 mm). For the numerical approximation of the integral in Formula (8), a sum with a diameter step of 0.5 mm was used (preliminary testing showed this step was small enough to ensure the convergence of the calculation). Rainfall intensities ranging from 5 to 200 mm.h^{-1} were considered, with a step of 5 mm.h^{-1}. A water depth h ranging from 0.25 to 12 mm (0.25 mm, 0.5 mm, 0.75 mm; and from 1 to 12 mm with a step of 1 mm) was considered. Water depths h smaller than 0.25 mm and larger than 12 mm were not studied because they led to numerical instabilities and boundary condition problems (Nouhou Bako et al., 2016). For a given raindrop diameter D, the calculations were limited to $h \leq 3D$ because it is known that no

detachment occurs for larger depth due to the protective effect of the water layer (Mutchler and Young, 1975; Wang and Wenzel, 1970).

4. With the R software (`https://www.r-project.org`, 2017-12-12), power law regressions over Formula (10) were calculated. From these power law regressions, the coefficient B was obtained for each water layer depth h. This allowed for comparing, for each erosive factor, the computed values of the erosivity exponent $B(h)$ with the ones of the literature. Using the same method, an exponential regression was calculated to describe the dependence of $B(h)$ with the water layer depth using $B(h) = \alpha_1 \exp(\alpha_2\, h)$. Previous work by Torri et al. (1987) have used such exponential relationship. Our preliminary tests confirmed that such an exponential relationship gives a better fit than linear or power relationships. The special case $B(h) = 1$ was treated similarly to estimate the function $G(h)$ included in Formula (11).

The above calculations were carried out for the four erosive factors, the three DSD laws and the four shear stress thresholds. Such a wide range of conditions would be difficult to investigate using laboratory or field experiments, underlining one advantage of the numerical approach.

3 Results and Discussion

The effects of the DSD law and the erosive factor on the erosivity exponent B are presented first, followed by the effects of the shear stress threshold. The special case of $B = 1$ is then reported: considering Formula (11), $G(h)$ was calculated for the four erosive factors, the full range of water depth and a zero shear stress threshold ($\tau_c = 0$ Pa).

3.1 Computed vs Literature-based Erosivity Exponents

As mentioned in Section 2.4, results were obtained for all the range of rainfall intensities, water layer depths, shear stress thresholds and DSD laws. In all cases, a coefficient of regression close to one (R^2=0.99) was obtained, confirming that a power law function is a suitable relationship between the erosive factors and the soil detachment rate (Meyer, 1981; Nearing et al., 1989; Smith and Wischmeier, 1957; Salles et al., 2000).

The values of the erosivity exponent B obtained for the intensity, the moment and the kinetic energy were compared with the experiment-based values found in the literature (Salles et al., 2000; Salles and Poesen, 2000; Nearing et al., 1989) (Figure 1). Such a comparison could not be carried out for MD because a range of values for this erosive factor could not be defined from the literature. Many computed values were within the literature-based range, showing a general agreement. However, a significant proportion of the computed values were lower than the literature-based range for I and M. For all the erosive factors, few computed values were in the top of the literature range. This discrepancy could be related to the approximation of the soil surface by a rigid plane in our simulations. It could also be related to the way the soil detachment is measured in the experiments. This point will be further discussed in Section 3.4.

3.2 Erosivity Exponent, Water Depth and DSD Laws

For the four erosive factors and taking $\tau_c = 0$ Pa, Formula (8) was solved for the whole ranges of water depth and rainfall intensity.

For the Marshal-Palmer law, the erosivity exponent B increased with the water depth in a similar manner for all the erosive factors (Figure 2). An identical behavior was observed for the other two DSD laws (graphs not shown).

The exponential regressions of the $B(h)$ curves are given in Table I. For a given DSD law, the values of the parameter inside the exponential were quite close to each other for all four erosive factors: about 0.053 for the Marshall-Palmer DSD law, 0.068 for the Gamma DSD law, and about 0.060 for the Lognormal DSD law. This is consistent with the parallelism of the curves (Figure 2). The values of the parameter in front of the exponential were not very far apart (between 0.66 and 0.88), but were always the lowest for MD (Table I, and, for the Marshall-Palmer law, Figure 2). For a given erosive factor, the parameters in front and inside the $B(h)$

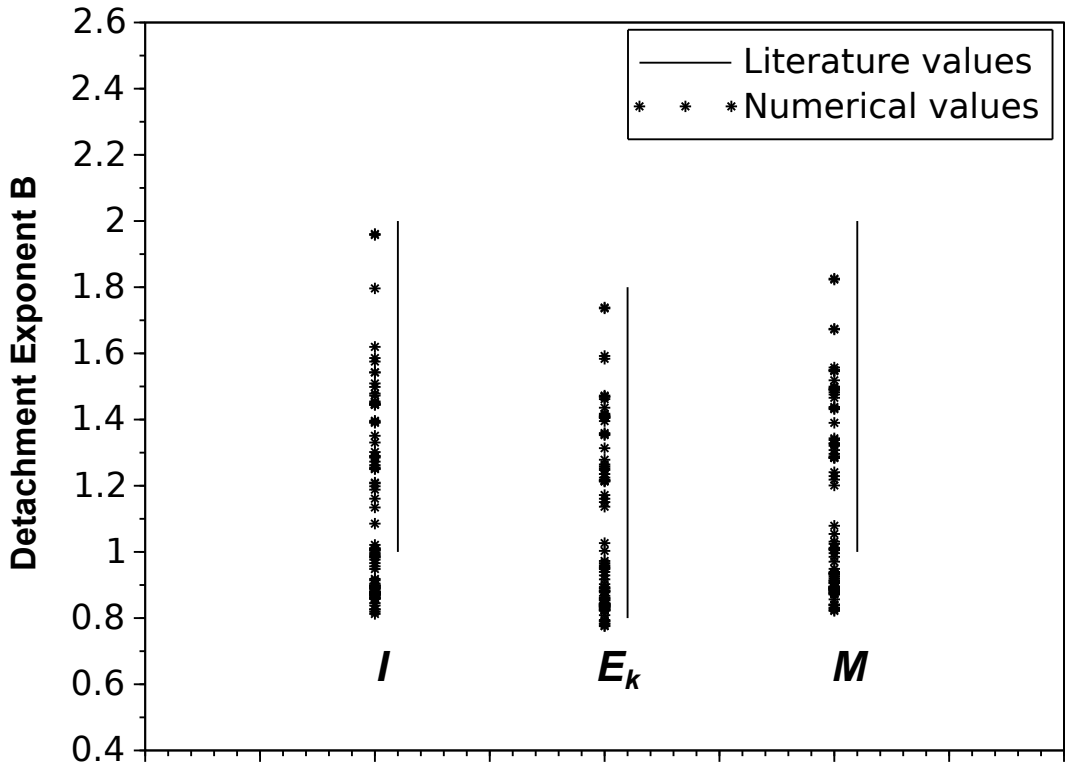

Figure 1: Comparison of the numerical values of the erosivity exponent B with the values taken from the literature for the intensity I, the kinetic energy E_k and the momentum M (Salles et al., 2000; Salles and Poesen, 2000; Nearing et al., 1989).

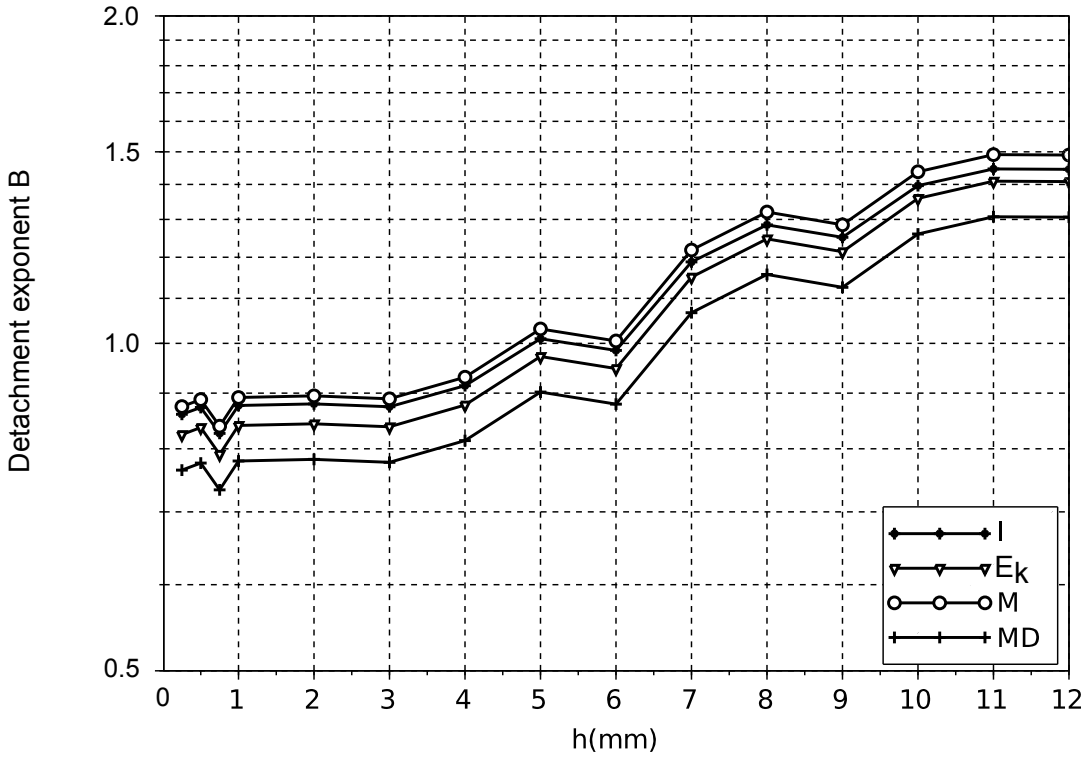

Figure 2: Evolution of erosivity exponent B as a function of the water depth h for the four erosive factors with the Marshall-Palmer law and $\tau_c = 0$ Pa. A log scale is used for the y-axis.

exponential were always the highest for the Gamma law (Table I). In the case of the erosive factor I, the relative difference of $B(h)$ between the Marshall-Palmer law and the Gamma law ranged from 10 % for h=0.25 mm to 30 % for h=12 mm (using the relationships given in Table I, see also Figure 3).

Table I: Exponential regressions for the erosivity exponent B as a function of the water depth h for the three drop size distributions laws and four erosive factors ($\tau_c = 0$ Pa).

	Marshall-Palmer ($R^2 = 0.95$)	Gamma ($R^2 = 0.95$)	Lognormal ($R^2 = 0.91$)
I	$0.80\exp(0.052h)$	$0.88\exp(0.068h)$	$0.78\exp(0.059h)$
E_k	$0.76\exp(0.054h)$	$0.78\exp(0.068h)$	$0.72\exp(0.061h)$
M	$0.81\exp(0.053h)$	$0.82\exp(0.068h)$	$0.76\exp(0.061h)$
MD	$0.71\exp(0.054h)$	$0.75\exp(0.068h)$	$0.66\exp(0.061h)$

While differences exists among the $B(h)$ relationships for the erosive factors and the DSD laws, they are small. This means that, in practice, the choice of a specific erosive factor may have a limited effect on the value of the erosivity exponent B (for a given DSD law). This will be especially true if experimental measurements are carried out to determine the $B(h)$ relationship: it is likely that the experimental errors (on the water depth, on the detachment, etc.) will alleviate finding large differences among the erosive factors. This may explain why ongoing discussions about the choice of the erosive factor (Salles et al., 2000; Usón and Ramos, 2001; Goebes et al., 2014) did not lead to a consensus. Moreover, the small differences found among the $B(h)$ regressions also shows that, when the erosive factors are calculated using formula (9), the erosivity exponent $B(h)$ is not sensitive to the chosen erosive factor. In practice, this means that any experimentally-determined value of $B(h)$ could be used with another erosive factor. This may lead to substantial simplifications for future modeling works: an erosive factor can be chosen based on the available data only (rainfall intensity, kinetic energy, etc.), without requiring extensive justification and testing. Additionally, the selection of an erosivity exponent $B(h)$ can be decided independently of the erosive factor.

Finally, the comparison of the results among DSD laws (Table I) confirms the findings of Parsons and Gadian (2000), who showed that the amount of soil detached by rain is influenced by the DSD law. Hence, the type of rain is likely to influence the value of the erosivity exponent B. Because the type of rain is location- and season-dependent, different erosive exponents may need to be used for a given modeling study.

From the experimental point-of-view, this suggests that more effort should be concentrated on the characterization of the rain and on the determination of the erosivity exponent $B(h)$ than on the determination of the most suitable erosive factor. Currently, most often, only rainfall intensity is reported in erosion studies. Kinetic energy and median drop size may also be given, but rarely with a confidence interval. And drop size distributions are quite rarely reported. This limits the value of data published in the literature: it is virtually impossible to decide for an erosivity exponent without better information about the rainfall properties.

3.3 Erosivity Exponent and Shear Stress Threshold

Previous results were obtained for a zero shear stress threshold ($\tau_c = 0$ Pa), meaning that any drop creating a shear stress at the soil surface caused some detachment. In this section, the effect of the shear threshold on $B(h)$ was analyzed for the four erosive factors considering four threshold values (τ_c=0, 0.25, 1 and 5 Pa). Note that $\tau_c = 5$ Pa is very large and out of the natural range, its only purpose being to bring out a potential effect of the shear threshold. Only the Marshall-Palmer law was considered here.

As shown by the high regression coefficients (Table II), in all sixteen cases (four shear stress thresholds times four erosive factors), exponential functions described well the dependence of the erosivity exponent B with the water layer depth h. For a given erosive factor, the regression parameters were similar, especially in the natural range of shear stress threshold. Only for $\tau_c = 5$ Pa, the parameter inside the exponential was slightly larger, leading to a larger value of the erosivity exponent B for large h. However, this difference remained limited (Figure 4). Owing for the extreme feature of a shear stress threshold of 5 Pa, it can be concluded that, in

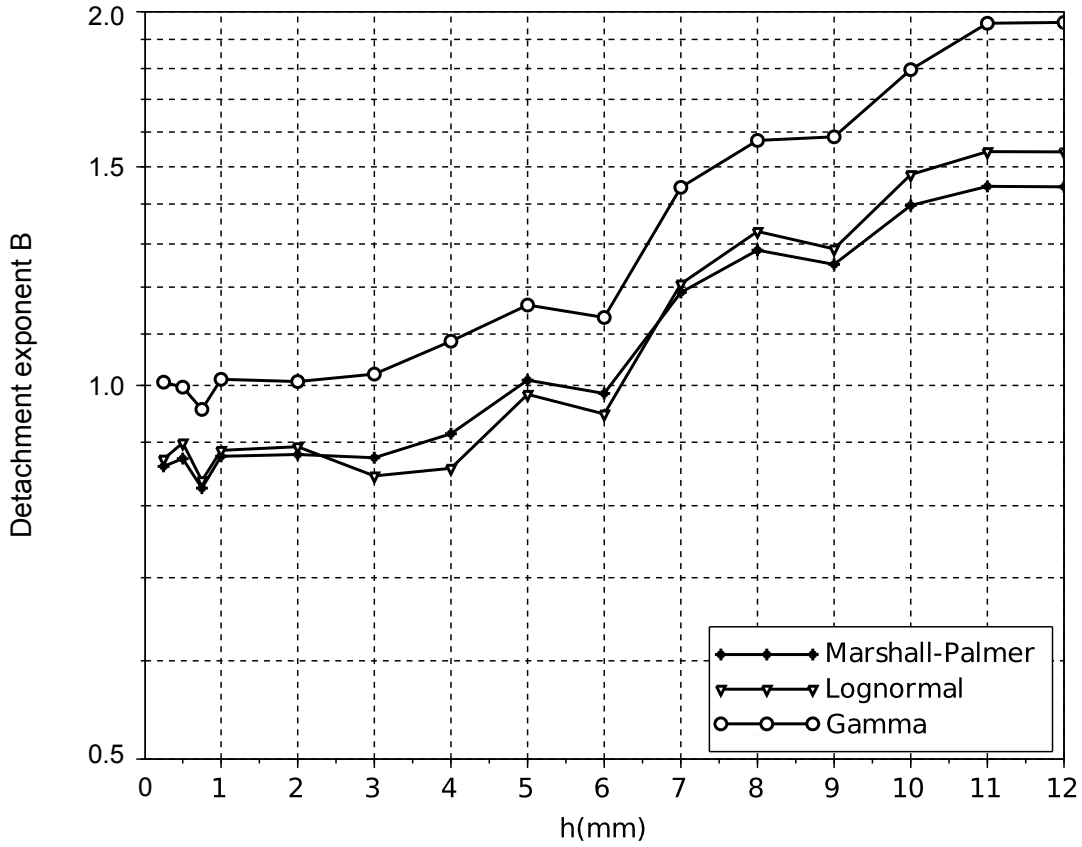

Figure 3: Evolution of erosivity exponent B as a function of the water depth h for the rainfall intensity I as erosive factor, and for the Marshall-Palmer, Gamma and Lognormal laws, with τ_c=0 Pa. A log scale is used for the y-axis.

the natural range, the shear stress threshold does not affect significantly $B(h)$. It means that soil mechanical properties, such as the particle size distribution or the soil cohesion, do not influence $B(h)$. This confirms the results of Beuselinck et al. (1999), who showed that the shear stress threshold is independent of the particle size. Moreover, it validates the usual practice of calibrating the erosivity exponent B independently of the soil, and hence to separate erosivity from erodibility.

Table II: Exponential regressions for the erosivity exponent B as a function of the water depth h for four shear stress values and the four erosive factors. The Marshall-Palmer law is considered.

	$\tau_c = 0$ Pa ($R^2 = 0.95$)	$\tau_c = 0.25$ Pa ($R^2 = 0.94$)	$\tau_c = 1$ Pa ($R^2 = 0.93$)	$\tau_c = 5$ Pa ($R^2 = 0.90$)
I	$0.80\exp(0.052h)$	$0.80\exp(0.053h)$	$0.79\exp(0.053h)$	$0.79\exp(0.059h)$
E_k	$0.76\exp(0.054h)$	$0.75\exp(0.055h)$	$0.76\exp(0.055h)$	$0.75\exp(0.061h)$
M	$0.81\exp(0.053h)$	$0.80\exp(0.055h)$	$0.80\exp(0.055h)$	$0.80\exp(0.061h)$
MD	$0.71\exp(0.054h)$	$0.70\exp(0.055h)$	$0.70\exp(0.055h)$	$0.70\exp(0.061h)$

For a given value of τ_c, the parameter inside the exponential was quite similar among the erosive factors. As in the previous section, the parameter in front of the exponential showed a limited spread, with the values for MD a bit separated from the others. This confirms the limited impact of the choice of the erosive factor on the erosivity exponent B.

It is remarkable that the purely numeric and physical approach used in the present work confirms past experimental studies. This encourages to pursue such approach to address additional issues in soil erosion, such as the processes of particle transport and sedimentation, and the effects of soil roughness, flow tortuosity, or crusting.

3.4 The Special Case $B = 1$, like in LISEM and EUROSEM

Considering Formula (11), the effect of the DSD law on $G(h)$ was analyzed for the four erosive factors. A zero shear stress threshold ($\tau_c = 0$ Pa) was used because previous results showed no effect of the threshold value.

Depending on the considered erosive factor, the ranges of $G(h)$ values were quite different, as shown by the differences in the scales of the y-axis (Figure 5). However, for all the erosive factors and all the DSD laws, a similar behavior was found, i.e. the general shape of the curves is similar. From $h = 0.25$ mm to $h = 4$ mm, $G(h)$ — and so the amount of soil detached by rain D_s — increased linearly with the water depth (Figure 5). A maximum of $G(h)$ was reached at $h = h_{D_s max} = 4$ mm. Then, for $h > 4$ mm, $G(h)$ decreased (and so the amount of rain-detached soil). This evolution can be explained by the nature of the shear stress created by the raindrop impacts. For low h (such as 0.25 mm), the water layer depth is thin enough to allow both small and large raindrops to contribute to soil detachment. However, in this situation, the shear stress has a short duration and a limited spatial extent due to the thinness of the water layer. This leads to intermediate values of $G(h)$, and hence to intermediate soil detachment D_s. As the water layer increases up to $h_{D_s max}$ (4 mm in the present simulations), the shear duration and its spatial extent increase, leading to an increase of D_s. Beyond the maximum value $h_{D_s max}$, the water layer protects the soil from the effect of small raindrops. Only large raindrops can contribute to the detachment of soil, but these raindrops are rare and their efficiency decreases as the water layer increases, leading to the decrease of D_s.

It must be stressed that the existence of a depth having a maximum detachment rate was not prescribed in the simulations. It is the process of detachment by raindrops itself that led to a critical depth of maximum detachment $h_{D_s max}$.

A critical depth has also been observed in the experiments of Moss and Green (1983) and Kinnell (1991). In a context of interrill erosion experiments, where detachment and sedimentation occur simultaneously, these authors found a maximum transport rate for a critical depth between 2 and 3 raindrop diameters. The experiments of Moss and Green (1983) and Kinnell (1991) involved more phenomena than the present simulations, and these phenomena could have complex feedbacks. Hence, the similarity in the values of the critical depth

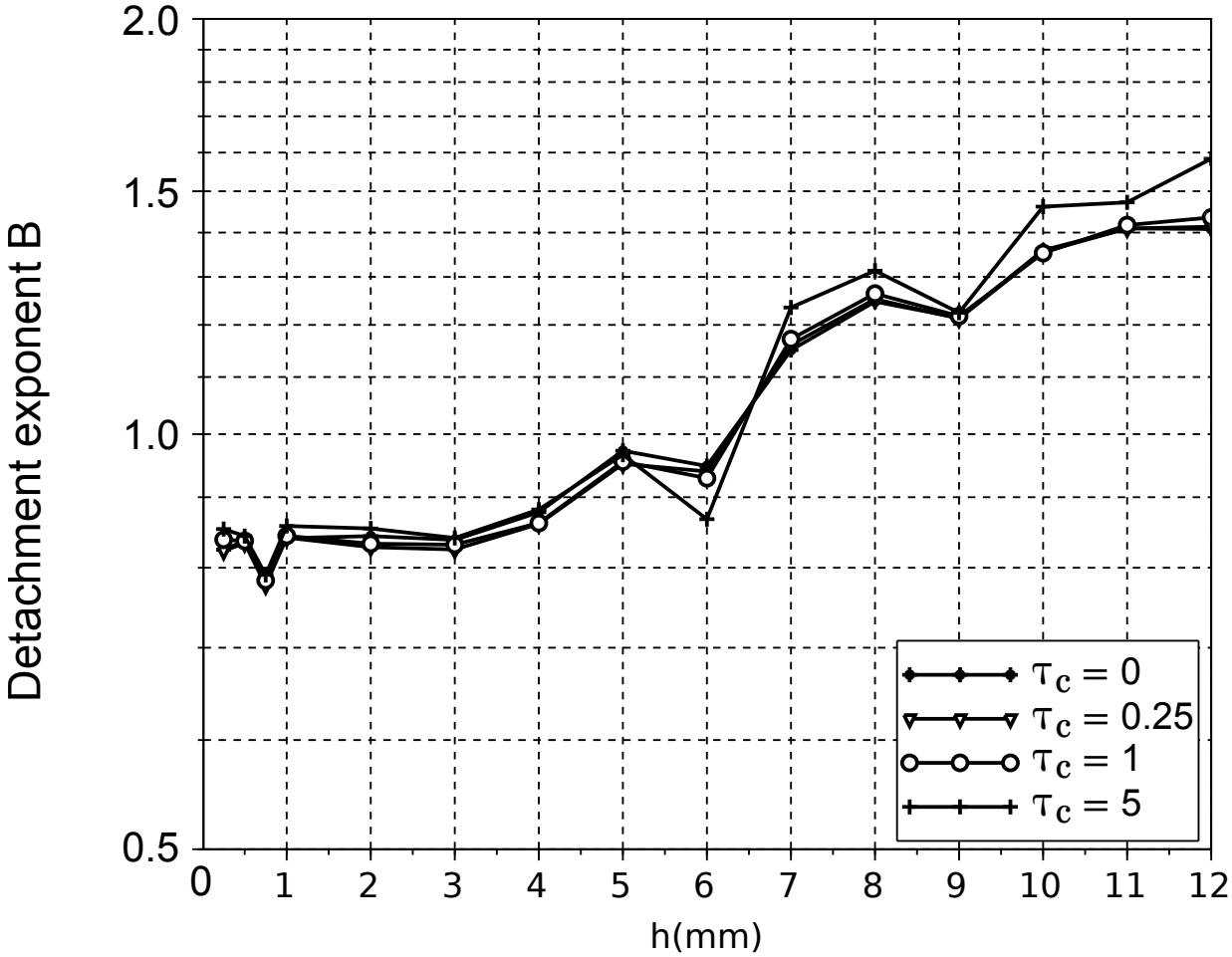

Figure 4: Evolution of erosivity exponent B as a function of the water depth h in the case of the rainfall kinetic energy E_k as erosive factor, for τ_c=0, 0.25, 1 and 5 Pa with the Marshall-Palmer law. A log scale is used for the y-axis.

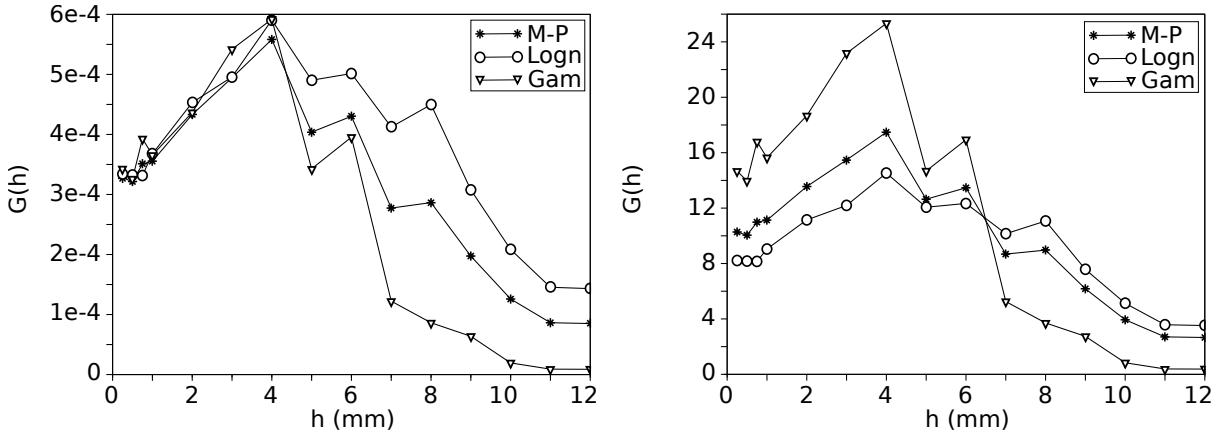

(a) Erosive factor I

(b) Erosive factor E_k

(c) Erosive factor M

(d) Erosive factor MD

Figure 5: Evolution of $G(h)$ depending on the water layer depth h for the four erosive factors and the three laws of drop size distributions (M-P: Marshall-Palmer. Logn: Lognormal. Gam: Gamma.), with $\tau_c = 0$ Pa.

could be a coincidence. Finding out if the critical depth reported by Moss and Green (1983) and Kinnell (1991) was caused by detachment only is out of the scope of the present study. However, including more processes is nowadays within the reach of computational fluid simulations. Pursuing further such an approach has the potential to lead to new insights about the mechanisms of raindrop-soil interactions.

When considering the effect of the DSD laws, differences were observed depending on the erosive factor (Figure 5). For the intensity I, the curves were superimposed for $h < 4$ mm. For $h > 4$ mm, $G(h)$ had the highest values for the Lognormal law and the lowest ones for the Gamma law (Figure 5a). For the other three erosive factors (E_k, M and MD), the Gamma law gave the highest values and the Lognormal the lowest ones up to $h \approx 6$ mm (Figures 5b, 5c and 5d). Above this value of h, the order of the curves were reversed. This shows the value of the $G(h)$ depends on both the type of rain and the considered erosive factor. As for the erosive exponent $B(h)$, the issue of the rainfall type shows up again. As previously stated, the rainfall type may have been an overlooked issue in previous studies: intensity is not a sufficient quantification of the rain. This reinforces the recommendation for more detailed description of rain properties (i.e. drop size distribution) in future experimental studies.

LISEM (De Roo et al., 1996) and EUROSEM (Morgan et al., 1998; Gumiere et al., 2009) described the water layer effect on soil detachment using the functions $G(h) = \exp(-1.48h)$ and $G(h) = \exp(-2h)$, respectively, with the kinetic energy E_k as erosive factor. The negative parameter means a continuous decrease of the detachment when the water depth increases. Hence, their functions do not include a maximum detachment, as observed experimentally (Moss and Green, 1983; Kinnell, 1991) and numerically (this study). This can be viewed as a simplification of the reality related to their modeling effort.

To account for this simplification, an exponential curve was fitted to the decreasing part of $G(h)$ for the specific case of kinetic energy E_k as erosive factor, using the Marshall-Palmer law and a zero shear stress threshold. The function $G(h) = \exp(-0.25h)$ was obtained (with $R^2 = 0.95$). This relation has a much lower parameter (-0.25) than the ones of LISEM and EUROSEM. In these models, the function $G(h)$ has been obtained from experimental studies (Torri et al., 1987; De Roo et al., 1996) which did not exactly quantified the amount of soil detached, but measured the amount of soil transported by splash (Fernández-Raga et al., 2017). There may be a bias in their $G(h)$ function because (1) the amount of splashed soil is a fraction of the amount of soil detached by raindrops, and (2) the proportion of the splashed soil decreases as the water layer depth increases (Ghadiri and Payne, 1988; Dunne et al., 2010; Schultz et al., 1985). Such bias could explain the discrepancy between the parameters of the function $G(h)$. This call for new experimental evaluations of the function $G(h)$. These experiments should be able to quantify the amount of detached soil, instead of the amount of splashed soil. This could be achieved only through new experimental designs.

Finally, it must be emphasized that all the results presented here are based on simulations of computational fluid dynamics. These results would have been quite difficult to get from field or laboratory experiments. Computational fluid dynamics has made enormous progress in the past decade, but have not benefited to soil erosion research, due probably to the fragmentation of scientific disciplines. The authors wish that the present paper will encourage other members of the scientific community to use computational fluid dynamics to the benefit of soil protection.

4 Conclusions

Using simulations of computational fluid dynamics, interrill erosivity was addressed. The erosivity exponent $B(h)$ was overall well-described by the simulations, although somewhat underestimated compared to the literature. This discrepancy could be related to the approximation of a rigid soil surface in the simulations or to an underestimation of soil detachment by splash measurements in the experiments.

The choice of the erosive factor had a minor effect on the erosivity exponent $B(h)$. Hence, although they have contrasted definitions, the erosive factors can be considered as equivalent for the purpose of relating the rainfall to the soil detachment. This may put an end to continuing arguments about the most appropriate erosive factor: Future studies may choose the most convenient erosive factor, and use erosivity exponent determined for another erosive factor. The threshold of the soil shear stress was found to have no effect on the erosivity exponent $B(h)$, confirming that this erosivity exponent is completely independent of the soil. This reinforces

the long-term practice of separating the erodibility of the soil and the erosivity of the rain.

The type of rain, i.e. the DSD law, had a major effect on the erosivity exponent $B(h)$ and on the function $G(h)$, meaning published values of $B(h)$ and $G(h)$ may be valid only for the type of rain they were designed for. Different $B(h)$ and $G(h)$ may have to be used for different rain types. This advocates for focusing future experimental research on the relationship between soil erosion and rainfall type. When determining erosivity exponent values, detailed rainfall properties should be given.

Considering the interaction between the shear stress dynamics and the protective effect of water layer, a depth having a maximum detachment rate was found. Using a decreasing exponential form for $G(h)$ showed discrepancy between previously-published functions and the present work. This calls for conducting experimental studies able to evaluate the amount of soil detached by raindrops — and not only the amount of splashed soil.

While it used a purely numeric and physical approach, the present work is in close match with past experimental studies. This demonstrates the large capabilities of computational fluid simulations. Other soil erosion issues could benefit from its use, especially for cases difficult to address experimentally.

References

Ariathurai, C. (1974). *A Finite Element Model for Sediment Transport in Estuaries*. PhD thesis, University of California, Davis, CA.

Assouline, S. (2009). Drop size distributions and kinetic energy rates in variable intensity rainfall. *Water Resources Research*, 45, DOI: 10.1029/2009WR007927.

Beuselinck, L., Govers, G., Steegen, A., and Quine, T. A. (1999). Sediment transport by overland flow over an area of net deposition. *Hydrological Processes*, 13:2769–2782.

Bradford, J. M., Ferris, J. E., and Remley, P. A. (1987). Interrill soil erosion processes — 2. Relationship of splash detachment to soil properties. *Soil Science Society of America Journal*, 51:1571–1575.

Brodie, I. and Rosewell, C. (2007). Theoretical relationships between rainfall intensity and kinetic energy variants associated with stormwater particle washoff. *Journal of Hydrology*, 340(1–2):40–47, DOI: 10.1016/j.jhydrol.2007.03.019.

Brodowski, R. (2013). Soil detachment caused by divided rain power from raindrop parts splashed downward on a sloping surface. *Catena*, 105:52–61, DOI: 10.1016/j.catena.2013.01.006.

Cugerone, K. and Michele, C. D. (2015). Johnson SB as general functional form for raindrop size distribution. *Water Resources Research*, 51(8):6276–6289, DOI: 10.1002/2014wr016484.

Cuomo, S., Chareyre, B., d'Arista, P., Della Sala, M., and Cascini, L. (2016). Micromechanical modelling of rainsplash erosion in unsaturated soils by discrete element method. *Catena*, 147:146–152, DOI: 10.1016/j.catena.2016.07.007.

De Roo, A. P. J., Wesseling, C. G., and Ritsema, C. J. (1996). LISEM: a single-event, physically based hydrological and soil erosion model for drainage basins. I: Theory, input and output. *Hydrological Processes*, 10(8):1107–1117, DOI: 10.1002/(SICI)1099-1085(199608)10:8<1107::AID-HYP415>3.0.CO;2-4.

Dunne, T., Malmon, D. V., and Mudd, S. M. (2010). A rain splash transport equation assimilating field and laboratory measurements. *Journal of Geophysical Research — Earth Surface*, 115:F01001–1–16, ISSN: 0148-0227, DOI: 10.1029/2009JF001302.

Ellison, W. D. (1944). Studies of raindrop erosion. *Agricultural Engineering*, 25(4, 5):131–136, 181–182.

Feingold, G. and Levin, Z. (1986). The lognormal fit to raindrop spectra from frontal convective clouds in Israel. *Journal of Climate and Applied Meteorology*, 25(10):1346–1363, ISSN: 0733-3021, DOI: 10.1175/1520-0450(1986)025<1346:TLFTRS>2.0.CO;2.

Fernández-Raga, M., Palencia, C., Keesstra, S., Jordán, A., Fraile, R., Angulo-Martínez, M., and Cerdà, A. (2017). Splash erosion: A review with unanswered questions. *Earth-Science Reviews*, 171:463–477, DOI: 10.1016/j.earscirev.2017.06.009.

Gabet, E. J. and Dunne, T. (2003). Sediment detachment by rain power. *Water Resources Research*, 39(1):1002, DOI: 10.1029/2001WR000656.

Ghadiri, H. and Payne, D. (1988). The formation and characteristics of splash following raindrop impact on soil. *Journal of Soil Science*, 39(4):563–575, ISSN: 0022-4588.

Gilley, J. E., Woolhiser, D. A., and McWhorter, D. B. (1985). Interrill soil erosion, part I: Development of model equations. *Transactions of the ASAE*, 28:147–153.

Goebes, P., Seitz, S., Geißler, C., Lassu, T., Peters, P., Seeger, M., Nadrowski, K., and Scholten, T. (2014). Momentum or kinetic energy – how do substrate properties influence the calculation of rainfall erosivity? *Journal of Hydrology*, 517:310–316, DOI: 10.1016/j.jhydrol.2014.05.031.

Gumiere, S. J., Le Bissonnais, Y., and Raclot, D. (2009). Soil resistance to interrill erosion: Model parameterization and sensitivity. *Catena*, 77(3):274–284, ISSN: 0341-8162, DOI: 10.1016/j.catena.2009.02.007.

Hall, R. L. and Calder, I. R. (1993). Drop size modification by forest canopies: Measurement using a disdrometer. *Journal of Geophysical Research*, 98:18465–18470.

Hartley, D. M. and Alonso, C. V. (1991). Numerical study of the maximum boundary shear-stress induced by raindrop impact. *Water Resources Research*, 27(8):1819–1826, ISSN: 0043-1397, DOI: 10.1029/91WR01219.

Hartley, D. M. and Julien, P. Y. (1992). Boundary shear-stress induced by raindrop impact. *Journal of Hydraulic Research*, 30(3):341–359, ISSN: 0022-1686.

Houwing, E. J. (1999). Determination of the critical erosion threshold of cohesive sediments on intertidal mudflats along the Dutch Wadden sea coast. *Estuarine Coastal and Shelf Science*, 49(4):545–555, DOI: 10.1006/ecss.1999.0518.

Kinnell, P. I. A. (1982). Laboratory studies on the effect of drop size on splash erosion. *Journal of Agricultural Engineering Research*, 27(5):431–439, ISSN: 0021-8634, DOI: 10.1016/0021-8634(82)90081-6.

Kinnell, P. I. A. (1991). The effect of flow depth on sediment transport induced by raindrops impacting shallow flows. *Transactions of the ASAE*, 34(1):161–168.

Lang, G., Schubert, R., Markofsky, M., Fanger, H.-U., Grabemann, I., Krasemann, H., Neumann, L., and Riethmuller, R. (1989). Data interpretation and numerical modeling of the mud and suspended sediment experiment 1985. *J. Geophys. Res.*, 94:14381–14393.

Low, T. B. and List, R. (1982). Collision, coalescence and breakup of raindrops. Part I: Experimentally established coalescence efficiencies and fragment size distributions in breakup. *Journal of the Atmospheric Sciences*, 39(7):1591–1606, ISSN: 0022-4928, DOI: 10.1175/1520-0469(1982)039<1591:CCABOR>2.0.CO;2.

Marshall, J. S. and Palmer, W. M. (1948). The distribution of raindrops with size. *Journal of Meteorology*, 5:165–166.

McLean, S. (1985). Theoretical modelling of deep ocean sediment transport. *Mar. Geol.*, 66:243–265.

Meyer, L. D. (1981). How rain intensity affects interrill erosion. *Transactions of the ASAE*, 24(6):1472–1475, DOI: 10.13031/2013.34475.

Morgan, R. P. C., Quinton, J. N., Smith, R. E., Govers, G., Poesen, J. W. A., Auerswald, K., Chisci, G., Torri, D., and Styczen, M. E. (1998). The European soil erosion model (EUROSEM): A dynamic approach for predicting sediment transport from fields and small catchments. *Earth Surface Processes and Landforms*, 23:527–544.

Moss, A. J. and Green, P. (1983). Movement of solids in air and water by raindrop impact. Effects of drop-size and water-depth variations. *Aust. J. Soil Res.*, 21:257–269.

Mouzai, L. and Bouhadef, M. (2011). Shear strength of compacted soil: effects on splash erosion by single water drops. *Earth Surface Processes and Landforms*, 36(1):87–96, DOI: 10.1002/esp.2021.

Mutchler, C. K. and Young, R. A. (1975). Soil detachment by raindrops. In *Present Prospective Technology for Predicting Sediment Yields and Sources. Proceedings of the Sediment-Yield Workshop, USDA Sedimentation Laboratory, Oxford, Mississippi, November 28-30,1972*, pages 114–117. Agricultural Research Service, U.S. Dep. of Agric.

Nanko, K., Moskalski, S. M., and Torres, R. (2016). Rainfall erosivity–intensity relationships for normal rainfall events and a tropical cyclone on the US southeast coast. *Journal of Hydrology*, 534:440–450, DOI: 10.1016/j.jhydrol.2016.01.022.

Nearing, M. A., Foster, G. R., Lane, L. J., and Finkner, S. C. (1989). A process-based soil erosion model for USDA-water erosion prediction project technology. *Transactions of the ASAE*, 32:1587–1593, DOI: 10.13031/2013.31195.

Nearing, M. A., Yin, S., Borrelli, P., and Polyakov, V. O. (2017). Rainfall erosivity: An historical review. *Catena*, 157:357–362, DOI: 10.1016/j.catena.2017.06.004.

Nouhou Bako, A., Darboux, F., James, F., Josserand, C., and Lucas, C. (2016). Pressure and shear stress caused by raindrop impact at the soil surface: Scaling laws depending on the water depth. *Earth Surface Processes and Landforms*, 41:1199–1210, DOI: 10.1002/esp.3894. DOI: 10.1002/esp.3894.

Nouhou Bako, A., Darboux, F., James, F., and Lucas, C. (2017). Raindrop interaction in interrill erosion: a probabilistic approach. *Water Resources Research*, 53(5):4361–4375, DOI: 10.1002/2017WR020568. DOI:10.1002/2017WR020568.

Parsons, A. J. and Gadian, A. M. (2000). Uncertainty in modelling the detachment of soil by rainfall. *Earth Surface Processes and Landforms*, 25:723–728.

Popinet, S. (2003). Gerris: a tree-based adaptive solver for the incompressible Euler equations in complex geometries. *J. Comp. Phys.*, 190(2):572–600.

Rose, C. W., Williams, J. R., Sander, G. C., and Barry, D. A. (1983). A mathematical model of soil erosion and deposition processes: I. Theory for a plane land element. *Soil Science Society of America Journal*, 47(5):991–995.

Salles, C. and Poesen, J. (2000). Rain properties controlling soil splash detachment. *Hydrological Processes*, 14(2):271–282.

Salles, C., Poesen, J., and Govers, G. (2000). Statistical and physical analysis of soil detachment by raindrop impact: Rain erosivity indices and threshold energy. *Water Resources Research*, 36(9):2721–2729, DOI: 10.1029/2000WR900024.

Sanchez-Moreno, J. F., Mannaerts, C. M., Jetten, V., and Löffler-Mang, M. (2012). Rainfall kinetic energy–intensity and rainfall momentum–intensity relationships for cape verde. *Journal of Hydrology*, 454-455:131–140, DOI: 10.1016/j.jhydrol.2012.06.007.

Sanford, L. P. and Maa, J. P.-Y. (2001). A unified erosion formulation for fine sediments. *Marine Geology*, 179:9–23.

Schultz, J. P., Jarrett, A. R., and Hoover, J. R. (1985). Detachment and splash of a cohesive soil by rainfall. *Transactions of the ASAE*, 28(6):1878–1884, ISSN: 0001-2351.

Sharma, P. P., Gupta, S. C., and Foster, G. R. (1993). Predicting soil detachment by raindrops. *Soil Science Society of America Journal*, 57(3):674–680, DOI: 10.2136/sssaj1993.03615995005700030007x.

Shin, S. S., Park, S. D., and Choi, B. K. (2016). Universal power law for relationship between rainfall kinetic energy and rainfall intensity. *Advances in Meteorology*, 2016:2494681, DOI: 10.1155/2016/2494681.

Smith, D. D. and Wischmeier, W. H. (1957). Factors affecting sheet and rill erosion. *Transactions, American Geophysical Union*, 38:889–896.

Torres, D. S., Porrà, J. M., and Creutin, J.-D. (1994). A general formulation for raindrop size distribution. *Journal of Applied Meteorology*, 33(12):1494–1502, DOI: 10.1175/1520-0450(1994)033<1494:agffrs>2.0.co;2.

Torri, D. and Sfalanga, M. (1986). Some aspects of soil erosion modeling. In Giorgini, A. and Zingales, F., editors, *Agricultural nonpoint source pollution: Model selection and application*, pages 161–171. Elsevier.

Torri, D., Sfalanga, M., and Sette, M. D. (1987). Splash detachment: Runoff depth and soil cohesion. *Catena*, 14(1–3):149–155, ISSN: 0341-8162, DOI: http://dx.doi.org/10.1016/S0341-8162(87)80013-9.

Ulbrich, C. W. (1983). Natural variations in the analytical form of the raindrop size distribution. *Journal of Climate and Applied Meteorology*, 22(10):1764–1775, DOI: 10.1175/1520-0450(1983)022<1764:NVITAF>2.0.CO;2.

Uplinger, W. G. (1981). A new formula for raindrop terminal velocity. In *Proceedings of the 20th Conference on Radar Meteorology*, pages 389–391, Boston, Mass. USA. American Meteorological Society.

Usón, A. and Ramos, M. (2001). An improved rainfall erosivity index obtained from experimental interrill soil losses in soils with a Mediterranean climate. *Catena*, 43(4):293–305, DOI: 10.1016/s0341-8162(00)00150-8.

Wang, R. C.-T. and Wenzel, Jr, H. G. (1970). The mechanics of a drop after striking a stagnant water layer. Technical Report 30, Water Resources Center, University of Illinois, USA.

Yin, S., Nearing, M. A., Borrelli, P., and Xue, X. (2017). Rainfall erosivity: An overview of methodologies and applications. *Vadose Zone Journal*, 16(12), DOI: 10.2136/vzj2017.06.0131.